J Mater Sci (2009) 44:1069–1075
DOI 10.1007/s10853-008-3203-z

Effect of austempering treatment on microstructure and mechanical properties of high-Si steel

D. Mandal · M. Ghosh · J. Pal · P. K. De · S. Ghosh Chowdhury · S. K. Das · G. Das · Sukomal Ghosh

Received: 8 August 2008 / Accepted: 17 December 2008 / Published online: 14 January 2009

Abstract In the present investigation, the influence of austempering treatment on the microstructure and mechanical properties of silicon alloyed cast steel has been evaluated. The experimental results show that an ausferrite structure consisting of bainitic ferrite and retained austenite can be obtained by austempering the silicon alloyed cast steel at different austempering temperature. TEM observation and X-ray analysis confirmed the presence of retained austenite in the microstructure after austempering at 400 °C. The austempered steel has higher strength and ductility compared to as-cast steel. With increasing austempering temperature, the hardness and strength decreased but the percentage of elongation increased. A good combination of strength and ductility has been obtained at an austempering temperature of 400 °C.

Introduction

The study of austempered ductile cast irons (ADI) is a world-wide hot point [1–3], as ADI shows excellent comprehensive mechanical properties explicitly higher strength and toughness when compared with ductile irons. The most notable limitation of ADI is the micro-segregation of some elements such as manganese and phosphorus, which induce brittleness. The other constraint is that the graphite nodules in the ADI act as 'crack source' and reduce service life of components under heavy abrasive wear and impact conditions. In recent years, the development of cast austempered steels gained interest in automobile industries because of unique combinations of properties achieved through alloying with inexpensive elements. Researches have been directed towards the study of austempered high-silicon cast steel having similar austempered structure (ausferrite structure) [1, 3]. This kind of steel shows better mechanical properties in respect of higher strength, hardness and toughness in comparison to ADI. It also exhibits higher life expectancy.

It is well known that conventional bainitic (austempered) structure is an aggregate of bainite and carbide. However, research reports indicate that the bainitic structure in high silicon containing steels consists of bainite plates and lath or interlath thin films of carbon-enriched retained austenite instead of carbide because silicon strongly retards the formation of carbide [4–7]. The carbon-enriched retained austenite undergoes strain-induced transformation to martensite [8, 9], greatly increasing the strain hardening rate, uniform elongation and the ultimate tensile strength. Therefore, the bainitic structure consisting of bainite and retained austenite is attractive in the development of high-strength steel with good ductility [7, 10, 11]. The amount of retained austenite present, after quenching from austenitising temperature, depends on the composition, cooling rate, austenite morphology, austempering temperature and time [12]. The formation of retained austenite, its morphology and influence on the mechanical properties have been studied by several investigators [7, 10, 11, 13]. Bhadeshia and Edmonds [7] reported that film like retained austenite was most desirable morphology to get good combination of strength and ductility. It had been reported that the austenite retention was especially promoted by addition of Mn that stabilised austenite and Si retarded cementite formation [14, 15].

D. Mandal (✉) · M. Ghosh · J. Pal · P. K. De · S. Ghosh Chowdhury · S. K. Das · G. Das · S. Ghosh
Metal Extraction and Forming Division, National Metallurgical Laboratory, Jamshedpur 831007, India
e-mail: durbadal73@yahoo.co.in; durbadal@nmlindia.org

Silicon is a good ferrite strengthener. Manganese content below 2% has a beneficial effect on hardenability, which contributes to solid solution strengthening. Simultaneous addition of small amount of micro alloying elements may further increase hardenability and precipitation strengthening.

The aim of this study is to develop high-silicon cast steel with microalloying addition and investigate the correlation between microstructure and mechanical properties of this steel at various austempering temperature.

Experimental procedure

In the present investigation, low-carbon high-silicon steels (10 kg heat) were prepared through induction melting. After melt down of low-carbon steels, Fe–Si, Fe–Mn and Fe–V were added in calculated amounts to achieve the composition of the steels. The chemical composition of the steel is shown in Table 1.

The cast blocks (120 mm × 90 mm × 38 mm) were homogenised at 1,000 °C for 6 h. The samples (120 mm × 90 mm × 8 mm) were austenitised at 900 °C for 30 min in a resistance heating furnace and subsequently quenched into a $NaNO_3$–KNO_3 salt bath capable of maintaining different austempering temperatures such as 350, 400 and 450 °C. The samples were isothermally held for 10 min followed by air-cooling. The samples were sectioned for microstructure analysis, hardness and tensile strength measurement.

The specimens were ground, polished and etched with nital (2%) solution for microstructure analysis. Optical and electron microscopy were used to study the microstructure of the specimens under different austempering conditions. The retained austenite volume fraction was determined by X-ray diffraction. The angular range (2θ) was 40°–130° with Cu Kα radiation at 40 kV with a scanning rate of 1° min^{-1}. Thin foil specimens were prepared for transmission electron microscopy (TEM) studies from 1-mm thick disc slit of austempered specimens. The discs were thinned down to below 100 μm by abrasion on 1,200 grade emery paper and then electro polished in a twin jet electro polisher using a mixture of 5% perchloric acid and 95% ethanol solutions at ambient temperature at about 50 V.

Hardness was measured with the help of Vickers hardness tester. A square-base diamond pyramid (included angle between the opposite faces of the pyramid is 136°) has been used as an indenter. The hardness was measured by applying 10-kg load for 15 s. Tensile tests were performed according to the ASTM standard method using 50T Instron machine at a constant strain rate of 0.5 mm min^{-1} at room temperature. At least two tensile samples were tested under similar condition. Fracture surfaces of broken tensile samples were observed under scanning electron microscopy to identify the mechanism of fracture of this alloy.

Table 1 Chemical composition of steel

Elements	C	Mn	Si	V	P	S	Fe
wt%	0.13	1.03	1.2	0.08	0.042	0.05	Bal.

Results and discussion

Optical microstructure analysis

As cast microstructure of steel (Fig. 1) shows a predominant ferrite matrix with pearlite dispersed in it. Figure 2a–c show the microstructure at various austempering temperatures (350, 400 and 450 °C) while the austenitising temperature (900 °C) and austempering time (10 min) remained constant. The austempered microstructure shows a matrix consisting of two phases. A dark etched bainite, which is of needle shape, and ferrite (white phase) are observed in the microstructure. Most of the bainites shown in these figures have lath morphology. It has been observed that the length of bainites remained almost equal with increasing austempering temperature yet width increased.

At lower transformation temperature, the bainite laths are finer and the orientation of lath is irregular. Increasing the austempering temperature from 350 to 450 °C, the bainitic ferrite laths widen and the carbon-enriched retained austenite between the adjacent bainite thickens. The initial stage of the transformation nucleates bainite at the austenite grain boundary that grows in parallel plates or

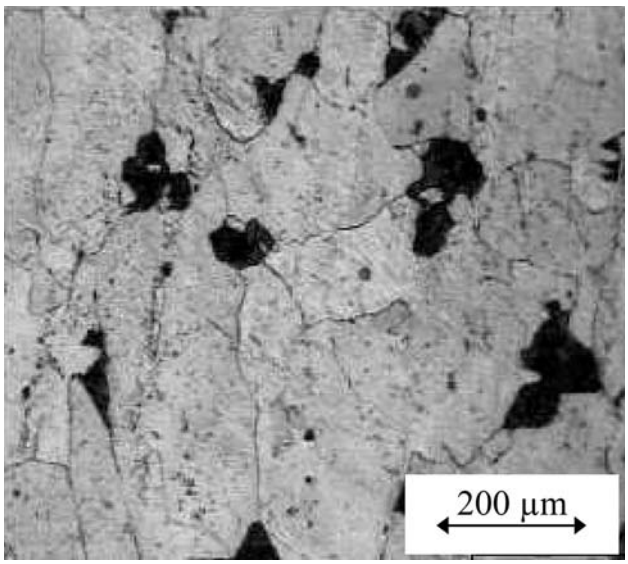

Fig. 1 Optical micrograph of the steel in as cast condition

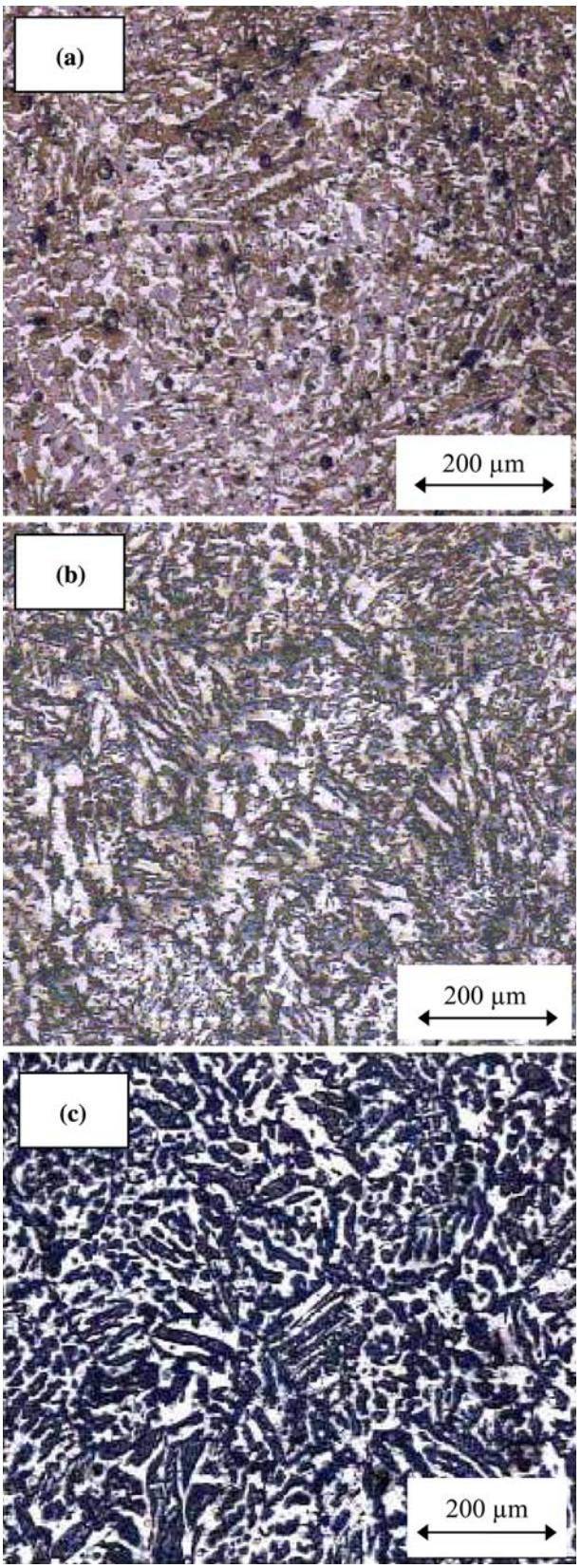

Fig. 2 Optical micrographs of steel isothermally transformed for 10 min at different temperatures: **a** 350 °C, **b** 400 °C and **c** 450 °C

laths (Fig. 2a) with rejection of carbon into the austenite. The microstructure of specimens, thus, reveals bainite and a low level of retained austenite. The structure shows higher strength but low toughness.

Some acicular bainite also have been observed at higher austempering temperature. The average length of lath and that of acicular ferrite are almost equal while these have different thickness. In other words, the morphology of bainite at the early stage of transformation is rather acicular and changes to lath-like morphology as a consequence of lateral growth as reported in the studies of austempered ductile iron [16]. The bainite formed at the beginning of transformation could have maximum lateral growth because those are surrounded by austenite having lower carbon content. The increase in carbon content of austenite is a consequence of the bainite decarbonisation that, in turn, reduces the driving force for lateral growth of bainite at the last stage of transformation. The results of the microstructural study show that austempering temperature has a minor effect on the bainite length while bainite width shows a pronounced variation with austempering temperature. It is assumed that sheaves of bainite form with an almost equal length and then lateral growth occurs.

TEM microstructure analysis

Bright field electron image (Fig. 3) shows general morphology of bainitic lath in a sample austempered at 350 °C. The bainitic lath is advancing parallel to the prior-austenite grain boundary and the packet of lower bainite sheaves originates from the prior-austenite grain boundary. The lath boundaries are slightly wavy and lack clarity due to their low-angle misorientation. The micrograph shows that the bainite sheaves are composed of smaller subunits of

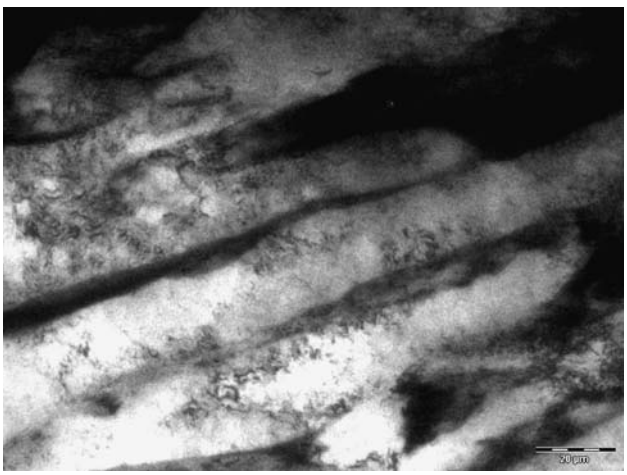

Fig. 3 TEM micrograph of the steel isothermally transformed at 350 °C for 10 min

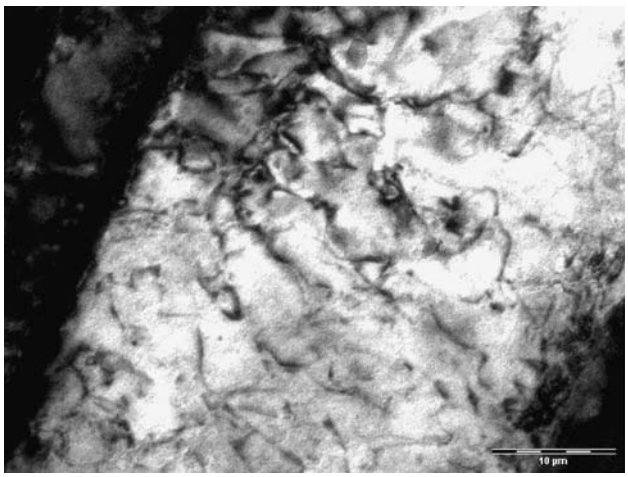

Fig. 4 TEM micrograph of carbide formation inside the bainite lath austempered at 350 °C for 10 min

bainite. In the packet of lower bainite, the widths of the subunits are very fine (25 μm) and reveal high angle lath boundaries. The interior decoration of a subunit has been elaborated through a magnified bright field electron image shown in Fig. 4, where the dislocation density in the lath is very high. The lower morphology of bainite subunit is due to carbon constraints imposed by the matrix commonly observed (shown in Fig. 4), such microstructure is a result of the displacive transformation mechanism.

In Fig. 5, the TEM photography shows a thin film of retained when austempered at 400 °C for 10 min. The presence of retained austenite is also confirmed through X-ray diffraction analysis. X-ray diffraction pattern is shown in Fig. 6. It is seen that the amount of retained austenite in this steel reaches a maximum of 6% at the isothermal transformation temperature of 400 °C and at a

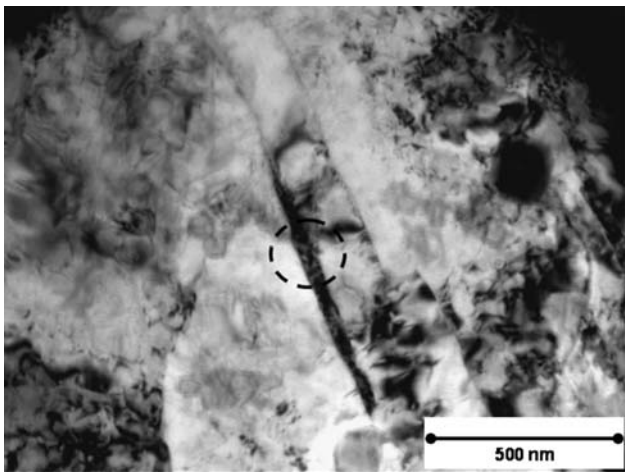

Fig. 5 TEM micrograph of the steel austempered at 400 °C: film-like retained austenite is visible between the bainite lath

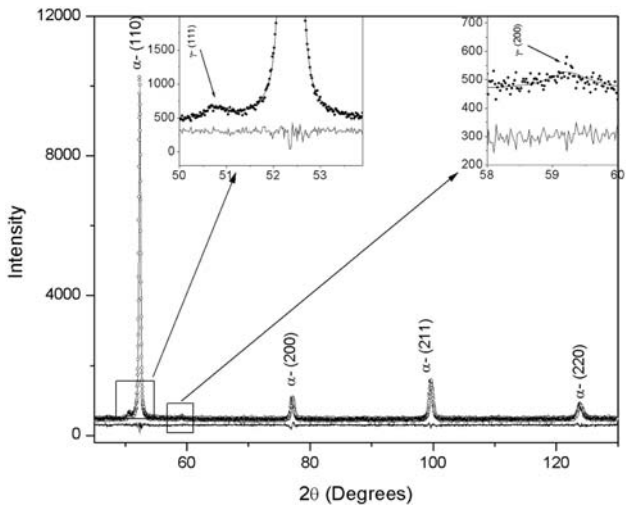

Fig. 6 XRD pattern of the steel austempered at 400 °C for 10 min

retention time of 10 min. It is well established that silicon inhibits the formation of cementite during bainite transformation and encourages the formation of carbon-enriched retained austenite [17] after partial transformation to bainite. The present high-carbon austenite did not transform completely to martensite.

The stability of this retained austenite is attributed to the high carbon and manganese content in the steel. Some of the austenite, adjacent to the grain boundaries transformed to bainite first after quenching at 400 °C in the salt bath, the formation of bainite caused the remaining austenite to be enriched with carbon. During isothermal transformation at 400 °C, bainite grew and the remaining austenite was further enriched with carbon. On cooling to room temperature, part of the austenite was retained, whereas the rest transformed into martensite. The retained austenite in the present isothermal transformed specimens was smaller in size than what was observed by the other investigators [13, 18]. Saleh and Priestner [13] observed that the width of retained austenite was a few microns in size and it was spaced uniformly in the bainite. In the present investigation, no carbides were identified in the structure because the presence of substantial amount of silicon delayed the cementite transformation from austenite. Silicon not only stabilised bainite in the austempered structure but also prohibited the formation of cementite.

Mechanical properties

Variation of mechanical properties with austempering Temperature:

The mechanical properties of high-silicon steel austempered at various austempering temperatures are shown in

Table 2 Mechanical properties of the steel at different austempering temperatures

Sample	Heat treatment Condition	Hardness (VHN)	UTS (MPa)	% El
Cast	Homogenised	183	553	21
35010	Austempered at 350 °C for 10 min	238	676	20
40010	Austempered at 400 °C for 10 min	224	663	27
45010	Austempered at 450 °C for 10 min	216	620	28

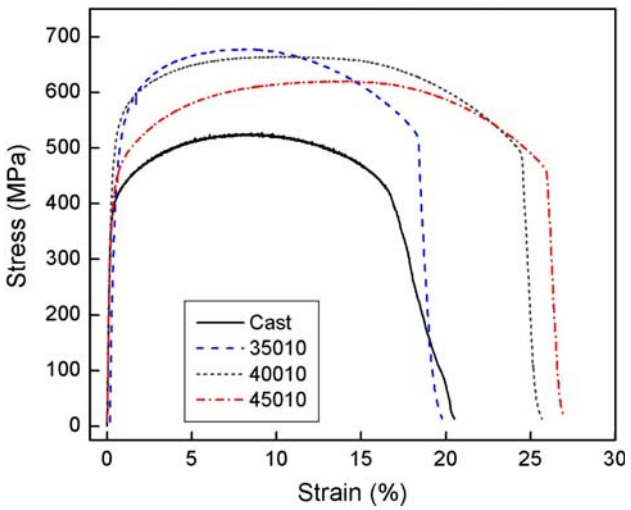

Fig. 7 Stress versus strain curves of the steel as cast condition and at different austempering temperatures

Table 2. Representative stress and strain curves are shown in Fig. 7. Ultimate tensile strength (UTS) of austempered steels is always higher compared to 'as-cast' steel. With an increase in austempering temperature, the tensile strength and hardness decreased and the percentage of elongation, an index of ductility, increased. The optimum combination of strength and ductility was obtained at an austempering temperature of 400 °C for 10 min of holding time. The steel showed high-tensile strength, high hardness and reduction in ductility when austempered at 350 °C. Also, with austempering at 450 °C, the steel revealed a higher percentage of elongation, but reduction in the UTS was observed.

The hardness and tensile strength of bainitic steel decrease with increasing austempering temperature. It is observed that the strength at any stage of interrupted tempering correlated well with the microstructure. These results imply that the strength depends mainly on carbide dispersion strengthening but unfortunately, the grain size, particle size and distribution of dislocation density are not independent parameters. It is an established fact that the combined strengthening effects of dislocation density and the ultrafine bainite grain size are very influential in the case of low-carbon bainitic steel. In bainite steel, retained austenite is responsible for the increase in ductility. Yield strength (YS), however, is found to be low due to the relative softness of the austenite.

Fracture surface analysis

The fracture surface morphology of the specimens austempered at different temperature and tested under monotonic tensile loading, is shown in Fig. 8a–c. The fracture surfaces of all the samples show cup and cone formation that indicate ductile fracture. It is observed that the dimple size increases but the number of dimples decreases with increasing austempering temperature. During tensile testing, initially some microvoids develop in the neck region. The microvoids usually nucleate at the regions of localised strain, discontinuity such as grain boundary, dislocation pile ups, second-phase particles inclusions etc. With increased strain, the microvoids grew, coalesced and eventually produced an internal crack by normal rupture.

The final separation of the materials occurred by shear rupture, which produced the wall of the cup and cone. Dimple rupture is the dominant mechanism of fracture as shown in Fig. 8. The size of the dimple is governed by the number and distribution of microvoids. When microvoids nucleate at the grain boundaries or at dislocation pile-ups, intergranular dimple rupture can occur. The maximum numbers of dimples on fracture surface are observed in samples those are austempered at 350 °C. Increase in austempering temperature enhances the dimple size by decreasing the number of dimples. The fracture exhibits numerous cup-like depressions caused by coalescence of microvoids.

The effects of austempering temperature on the strength and ductility are shown in Fig. 7. The specimens were austempered at different temperatures and were kept at an identical holding time (10 min). Therefore, any change in the mechanical properties should be due to the effect of tempering temperature only. Figure 7) shows that the highest UTS is obtained at 350 °C, but the percentage of elongation is low. The highest percentage of elongation is observed at 450 °C austempering temperature with a low strength. A good combination of UTS and percentage of elongation is observed at an austempering temperature of 400 °C and 10 min holding time. The microstructures of the austempered steel mainly govern the mechanical properties. The high strength at low-austempering temperature (350 °C) is associated with the formation of high strength lower bainite, which features dominantly in the structure.

The strength is mainly influenced by the carbon content in the bainite and the thickness of the bainitic laths. The

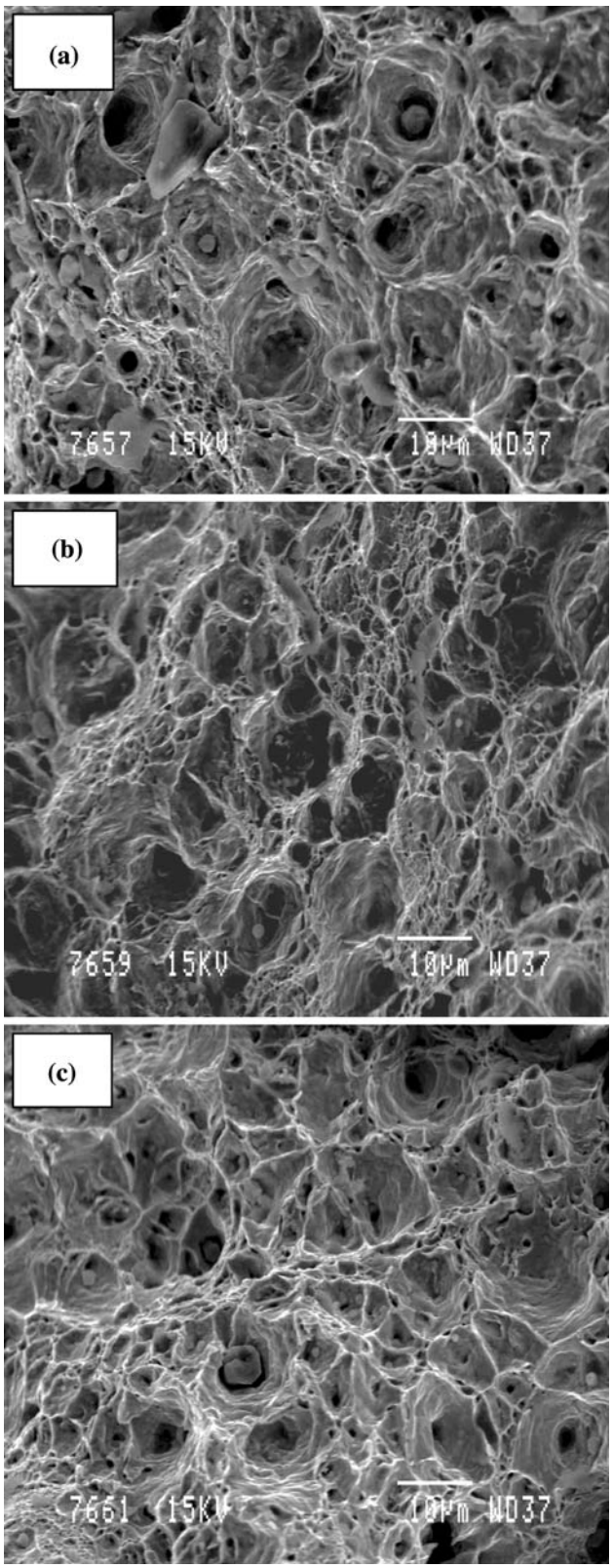

Fig. 8 SEM fractography of the steel austempered for 10 min at different temperatures: **a** 350 °C, **b** 400 °C and **c** 450 °C

ductility (%El) of the steel is principally decided by the sub-structure of the bainite lath and the quality and morphology of the carbon enriched retained austenite occupied between bainite laths [19]. In other words, the mechanical properties of the bainitic structure mainly depend on the diffusion of carbon during bainite transformation. At a lower transformation temperature (350 °C), the bainite laths become finer and close-net as shown in Fig. 2a, the amount of retained austenite is low. TEM studies have revealed the presence of carbides in the bainite lath at the austempering temperature of 350 °C as shown in Fig. 4. The microstructure results higher strength and hardness but accounts for reduction in the percentage of elongation or ductility.

The strength is also increased by impeding dislocation motions. The factors, which contribute to this aspect, include the fine structure of the bainite platelets, dispersed carbide formation and high-dislocation density. A low level of retained austenite was observed, originating from untransformed austenite, contributed to the low ductility at 350 °C austempering temperature. There is evidence [20] that the lower bainite generated after low-temperature transformation contains a concentration of carbon, which is located at defects such as dislocations within the ferrite lattice. The majority of dislocations in bainite are believed to be mobile, since sharp yield points are not observed during tensile tests.

With increase in austempering temperature, the morphology of bainite changes from fine to coarse (carbide free upper bainite). As a result, the strength is reduced and the ductility is increased. As the transformation temperature increases, the diffusion ability of the carbon atom increases and the degree of super cooling of the bainite transformation decreases. All these factors reduce the amount of the bainite laths, widen the laths, reduce the strength and the hardness and increase the ductility. At a higher austempered temperature (450 °C), the structure becomes coarse as shown in Fig. 2c, on the contrary, the dimple size on fracture surface increases (Fig. 8c), which results in increased ductility.

Conclusions

1. The microstructure of Fe–1.2Si–1.0Mn–0.08 V steel consists of bainitic ferrite and carbon-enriched retained austenite after austempering at different austempering temperatures.
2. The film-like retained austenite is observed when the isothermal transformation temperature is low, whereas blocky morphology of retained austenite appears when the temperature was high.

3. Austempering improves mechanical properties of high-silicon steel. With decrease in austempering temperature, the YS and the UTS are increased yet the ductility is decreased. The optimum combination of strength and ductility has been obtained (specimen specific) at an austempering temperature of 400 °C and 10 min holding time.
4. The fracture mechanisms of austempered steel are dominated by cup and cone formation, a feature of the ductile fracture. Dimple size increased with increasing austempering temperature, which indicates improvement in ductility.

References

1. Putatunda SK (2003) Mater Des 24:435
2. Hamid AS, Elliott R (1996) Mater Sci Tech 12(8):679
3. Li Y, Chen X (2001) Mater Sci Eng A308:277
4. Edmonds DV, Cochrane RC (1990) Metall Trans A 21:1527
5. Lee YK, Shin HC, Jang YC, Kim SH, Choi CS (2002) Scr Mater 47:805
6. Mirak AR, Nili-Ahmadabadi M (2004) Mater Sci Tech 20:897
7. Bhadeshia HKDH, Edmonds DV (1983) Met Sci 17:420
8. Daber S, Ravishankar KS, Prasad Rao P (2008) J Mater Sci 43:4929. doi:10.1007/s10853-008-2717-8
9. Daber S, Prasad Rao P (2008) J Mater Sci 43:357. doi:10.1007/s10853-007-2258-6
10. Matsumura O, Sakuma Y, Takechi H (1987) Trans ISIJ 27:570
11. Sugimoto KI, Ida T, Sakaguchi J, Kashima T (2000) ISIJ Int 40:902
12. Neves EG, Barbosa RN, Pereloma EV, Santos DB (2008) J Mater Sci 43:5705. doi:10.1007/s10853-008-2902-9
13. Saleh MH, Priestner R (2001) J Mater Proc Tech 113:587
14. Matlock DK, Krauss G, Speer JG (2001) J Mater Process Tech 117:324
15. Bailey AJ, Krauss G, Thomson SW, Szilva WA (1996) In: Proceedings of the 37th mechanical working and steel processing conference. ISS, Warrendale, PA, p 455
16. Nili Ahmadabadi M (1998) Metall Mater Trans A 29:2297
17. Bhadeshia HKDH (1980) Acta Metall 28:1103
18. Kim SW, Kim SH (1991) J Korean Inst Met Mater 29(10):967
19. Qu J, Yang D (1992) J Iron Steel Res 4(2):45
20. Bhadeshia HKDH, Waugh RW (1982) Acta Metall 30:775